Vortex Models for the Control of Flows

A.C. Smith[1]
acsmith@bu.edu

and

J. Baillieul[2]
Aerospace/Mechanical Engineering
Boston University
Boston, MA 02215
johnb@bu.edu

Abstract

There are a number of essential ingredients which must be brought together in order to develop a model-based control theory of boundary flows. In any such theory, models of fluid dynamics must (i) be simple enough to run in real-time, and (ii) be able to capture the physics of control actuator interaction with the fluid. Active vortex generators are one interesting candidate class of actuators which may be used together with vortex models or panel methods to broaden our understanding of flow separation control in various applications settings. While these methods offer the hope of modeling the essential aspects of the boundary flows with reasonable fidelity, their use in applications will require new (hybrid model based) approaches to simulation and control.

1 Introduction

There are many reasons for interest in controlling separation of the boundary layer over an airfoil. Effective control of separation can improve lift, reduce drag, and lessen turbulent velocity fluctuations, leading to improvements in performance and safety. Previous experimental work has shown that the use of pulsed-jet actuators at the leading edge of an airfoil can exert significant control over the separation of flow at high angles of attack [5].

An effective model-based theory of this type of control requires a model of the separation dynamics that accurately captures the physics of interaction between the actuator and the fluid while being simple enough to run in real time. One promising avenue for creating such a model is the use of point vortex methods. In these methods, vortices are treated as particles that influence each other in an otherwise irrotational, inviscid flow.

This paper presents an attempt to develop a point-vortex based model of separation dynamics that meets the accuracy and simplicity requirements for real-time control.

2 The model

The method used to model flow in two dimensions is a C^0 panel method. The flow is treated as a *complex potential* flow. The complex potential w is given by

$$w(z) = \phi(z) + i\psi(z)$$

where ϕ is a real potential function, ψ is a real stream function, and z is the complex coordinate $x + iy$. The functions ϕ and ψ are conjugates, i.e., they satisfy the Cauchy-Riemann equations:

$$\frac{\partial \phi}{\partial x} = \frac{\partial \psi}{\partial y}, \frac{\partial \phi}{\partial y} = -\frac{\partial \psi}{\partial x}.$$

This condition guarantees that w is analytic.

The fluid velocity at a point z is given by

$$u - iv = \overline{u + iv} = \frac{\partial w}{\partial z},$$

where u and v are the x- and y-components of velocity, respectively, and the overline signifies complex conjugation. Note that the complex velocity $u + iv$ is the complex conjugate of $\partial w/\partial z$. Any valid complex potentials can be superimposed or scaled as necessary.

[1]Support for A.C. Smith from the United Technologies Corporation is gratefully acknowledged.

[2]Support from the Army Research Office under the ODDR&E MURI97 Program Grant No. DAAG55-97-1-0114 to the Center for Dynamics and Control of Smart Structures (through Harvard University) is gratefully acknowledged.

2.1 Flow components

The complex potential for a point vortex of strength Γ at a point z_0 is given by

$$w = \frac{\Gamma}{2\pi} \log(z - z_0),$$

which gives a velocity field of

$$u - iv = \frac{\Gamma}{2\pi(z - z_0)}. \tag{1}$$

A vortex in a flow field will be convected by all external flow elements. Thus, for a family of n vortices with locations z_i and strengths Γ_i, the motion of the individual vortices is described by

$$\overline{\left(\frac{\mathrm{d}z_i}{\mathrm{d}t}\right)} = \Sigma_{j \neq i}^{n} \frac{\Gamma_i}{2\pi(z_i - z_j)}.$$

The complex potential for a uniform flow with constant velocity components U and V in the x- and y-directions is

$$w = (U - iV)z.$$

2.2 The panel method

The contribution to the flow field made by the airfoil is determined by applying a C^0 panel method. The surface of the airfoil is modeled as a set of node points connected by line segments, or *panels*. Each panel is considered to have a distributed surface vorticity that varies linearly along the length of the panel. The surface vorticity is continuous from panel to panel, though not smoothly so. Thus, the distribution of surface vorticity is determined by the densities at the node points.

At any point in time, these densities are determined by applying a non-penetration condition to the surface of the airfoil. The non-penetration condition is implemented by requiring that the net mass flux through each panel of the body surface be zero.

At any location z, the fluid velocity $\overline{\mathrm{d}w/\mathrm{d}z}$ is linearly dependent on the vorticity density at each node point. Hence, the fluid flow through each panel is linearly dependent on these values as well. Thus, we need to find a solution to the system

$$\mathbf{A} \begin{bmatrix} \gamma_1 \\ \gamma_2 \\ \gamma_3 \\ \vdots \\ \gamma_{N-1} \\ \gamma_N \end{bmatrix} = F_d - F_{ext} \tag{2}$$

where

- $\mathbf{A}$ is a square matrix expressing the relationship between the vorticity densities at the node points and the fluid flux through the body panels,
- γ_i is the density of surface vorticity at node point i,
- N is the number of body panels (and hence the number of node points),
- F_d is a vector containing the desired flux through the body panels (in this case, a vector of N zeroes.)
- F_{ext} is a vector containing the flux through the body panels due to external conditions (e.g., the free stream, external point vortices, etc.).

In the absence of fluid sources or sinks, the total mass flux through a closed curve (such as the body surface) must be zero. Hence the vectors F_d and F_{ext} only have dimension $N - 1$, and eq. 2 cannot be used to fully determine the values γ_i. In order to make the system fully deterministic, we add an equation for the value of the stream function ψ at one of the node points. Thus,

$$\mathbf{A}' \begin{bmatrix} \gamma_1 \\ \gamma_2 \\ \gamma_3 \\ \vdots \\ \gamma_{N-1} \\ \gamma_N \end{bmatrix} = \begin{bmatrix} F'_d - F'_{ext} \\ \\ \psi_d - \psi_{ext} \end{bmatrix} \tag{3}$$

where

- $\mathbf{A}'$ is identical to $\mathbf{A}$ except that the bottom row has been replaced by a set of coefficients expressing the relationship between the γ_i values and the stream-function at one of the node points,
- F'_d and F'_{ext} are vectors containing the first $N-1$ elements of F_d and F_{ext} respectively.
- ψ_d is the desired stream function value at the specified node point,
- ψ_{ext} is the value of the stream function at the specified point due to external factors.

The value of ψ_d at any point in time is determined by the current Kutta circulation of the airfoil, i.e., the total vorticity in the airfoil's boundary layer. The value ψ_d is set such that the integral of vorticity around the airfoil's surface is equal to the Kutta circulation.

2.3 Diffusion and Vortex shedding

Diffusion of vorticity is handled stochastically. At each time-step of the integration process, all vortices are given random displacements δ_x and δ_y. These displacements have Gaussian distribution with mean and standard deviation

$$\overline{\delta_x} = \overline{\delta_y} = 0 \quad \sigma_{\delta_x, \delta_y} = \sqrt{2\Delta t / \mathrm{Re}}. \tag{4}$$

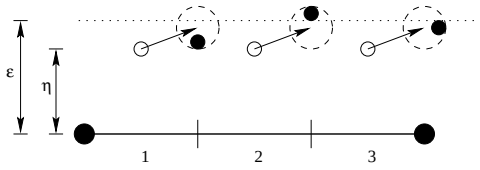

Figure 1: An abstraction of the vortex shedding scheme. The figure shows one panel with three subpanels. The open dots are the starting points of the trial vortices, the arrows represent the convection of the vortices over one time step, the dashed circles show the viscous (stochastic) diffusion of the vortices, and the solid dots show the final positions. In this diagram, the central vortex escapes the control zone (shown by the dotted line) and persists through subsequent time-steps; the other two vortices are re-absorbed into the surface viscosity.

where Δt is the time-step of the integration and Re is the Reynolds number of the flow ($\mathrm{Re} = U \cdot d/\nu$, where U is free-stream flow speed, d is a characteristic length, and ν is kinematic viscosity.)

The integration method used is an Adams-Bashforth second-order method. For each vortex i,

$$\begin{aligned} z_i(t_0 + \Delta t) &= z_i(t_0) \\ &+ \left[\frac{3}{2}\frac{\mathrm{d}z_i}{\mathrm{d}t}_{(t_0)} - \frac{1}{2}\frac{\mathrm{d}z_i}{\mathrm{d}t}_{(t_0-\Delta t)}\right]\Delta t \\ &+ (\delta_x + i\delta_y)\,, \end{aligned} \tag{5}$$

where Δt is the time-step of the integration.

The transfer of vorticity from the airfoil surface to the free stream is handled by allowing individual vortices to be shed from the boundary layer. The method used here is adapted from Lin, et. al. [6], and involves creating "trial vortices" within the airfoil's boundary layer and allowing some of these vortices to escape the surface vorticity layer through convection and diffusion.

A *control zone* is prescribed around the airfoil, with boundaries set a specified distance ϵ from the airfoil surface. The control zone is considered to represent the region in which airfoil's surface vorticity resides.

Each panel of the airfoil surface is broken into a number of subpanels. For each subpanel, at each time-step of the integration, a trial vortex is created a distance $\eta < \epsilon$ from the panel surface. The strength of the trial vortex is equal to the total surface vorticity distributed along the subpanel. Effectively, each trial vortex represents the possibility of the surface vorticity of its subpanel diffusing into the free stream.

The trial vortices are convected for one time-step using Euler's integration method, together with a random displacement (δ_x, δ_y) where (δ_x, δ_y) are bivariate normal random variables distributed as in Eq. 4 (Figure 1.) Thus for each trial vortex,

$$\begin{aligned} z_i(t_0 + \Delta t) &= z_i(t_0) + \frac{\mathrm{d}z_i}{\mathrm{d}t}_{(t_0)}\Delta t \\ &+ (\delta_x + i\delta_y)\,. \end{aligned} \tag{6}$$

The position of the vortex is then evaluated to determine whether the vortex has "escaped" into the free stream. If the position $z_i(t_0+\Delta t)$ lies outside the airfoil control zone, the vortex will persist through subsequent time steps, during which it will be treated like any other free-stream vortex, governed by eq. 5. If the position $z_i(t_0 + \Delta t)$ lies within the control zone, the vortex is eliminated and its vorticity is re-absorbed by the airfoil surface vorticity.

Finally, free-stream vortices are not guaranteed to remain free. Any free-stream vortex that re-enters the control zone is re-absorbed into the surface vorticity, just like a trial vortex.

Over most of the airfoil surface, the direction of flow near the foil surface will be nearly parallel to the surface, and hence nearly parallel to the control zone boundary. Thus, the escape of vortices from the control zone, as well as any subsequent recapture, will depend greatly on the stochastic diffusion, with the small component of flow velocity normal to the surface serving to increase or decrease the possibility of a trial vortex diffusing out of the control zone. Very rarely, if ever, will a trial vortex be convected out of the control zone by the bulk flow.

This method depends on simulating vorticity diffusion by means of random movement of point vortices. Because of this, it should be noted that the method may not work well in all cases. In particular, low Reynolds number flows are not well-simulated, because in these cases viscous diffusion of vorticity tends to dominate other effects. In such cases, the density of vortices decreases with time away from the control zone and the flow is not uniformly well approximated by the point vortex model. It is remarkable that at higher Reynolds numbers, coherent structures appear (as described in the next section). In this case, the density of vortices in the coherent structures tends to remain constant over time.

2.4 Computational issues

The procedure for computing one time-step of the simulation is:

1. Calculate the new positions of all free-stream vortices (eq. 5.)
2. Create trial vortices for the subpanels and determine their positions at the end of the time-step (eq. 6.)

3. Eliminate any vortices within the control zone and return their vorticity to the airfoil surface.

In most cases, the first step is the most computationally intensive. Conceptually, the simplest method for evaluating eq. 5 is to directly compute the influence of each vortex on every other vortex. This requires time $O(n^2)$, where n is the number of vortices.

The current method for evaluating eq. 5 is adapted from Barnes & Hut [1] and involves grouping vortices that are close to each other into clusters. A hierarchy of clusters is established, with small clusters belonging to larger clusters. The influence on a vortex of a sufficiently distant cluster can be approximated to a desirec accuracy without the necessity of examining each vortex within the cluster. This reduces the computational load to $O(n \log n)$.

In order to further lessen the computation required, a method for merging vortices is used. Two nearby vortices may be merged into a single vortex if the difference between the induced velocity field at the body surface before and after merging is less than some threshold. As a result, vortices near the body generally remain distinct, while vortices in the wake will often be merged.

Because the fluid velocity generated by a point vortex approaches infinity as the point of interest approaches the vortex, care must be taken to ensure that the resulting stiffness of the system does not introduce large errors into the simulation. There are several ways to handle this stiffness:

1. Use an integration scheme with an adaptive stepsize. This is impractical for our purposes because the step-size used must be small enough to accurately handle the closest pair of vortices in the wake. Since distances between vortices and their nearest neighbors vary widely throughout the wake, the vast majority of vortices will not require small-stepsize treatment, but the necessity of using the same (small) stepsize across the entire space will force the entire computation to slow down.

2. Replace the point-vortex model with a "vortex blob" model by replacing eq. 1 with

$$u - iv = \frac{\Gamma}{2\pi} \frac{\overline{(z - z_0)}}{|z - z_0|^2 + \sigma^2},$$

where σ is a "core radius" of the blob. This eliminates the singularity at the center of the vortex.

3. Employ a method for merging nearby vortices. This method assumes that when two vortices approach each other closely enough, they will coalesce into a single vortex. This is the method we are using.

3 Results

3.1 Cylinder

The first case investigated was that of two-dimensional flow past a cylinder. The cylinder was given a unit diameter and the free-stream was set to uniform velocity, thus giving $\mathrm{Re} = 1/\nu$.

Figure 2 shows a series of snapshots of the simulation. The most noteworthy feature visible is the formation of coherent vortex structures in the wake of the cylinder. As time flows and the wake develops, clockwise vortex clusters are shed alternately with counterclockwise clusters. This agrees qualitatively with often-repeated experimental results [2], and provides some assurance that this method captures important aspects of the physics of vorticity shedding.

3.2 Airfoil

Figure 3 shows the simulated flow past a Clark-Y airfoil at an angle of attack $\alpha = 0.25$rad. Airfoil chord length and freestream flow speed are both unity so, as for the cylinder simulations, $\mathrm{Re} = 1/\nu$. For these simulations, a Reynolds Number of 1.5×10^5 was used. The airfoil is instantaneously accelerated from rest with attitude held constant.

At time $t = 0.50$, a large amount of vorticity has been shed from the trailing edge of the wing – an expected effect of an instantaneous start from rest. Also, a build-up of vorticity is beginning to appear on the upper surface of the wing near the leading edge. At time $t = 1.50$, a large structure of clockwise vorticity has begun to detach from the surface. The effect of the vortex merging process is apparent at the downstream end of the wake, where several vortices have been merged to save computation time.

At later times, vortex shedding continues. In the last two snapshots, at times $t = 5.0$ and $t = 10.0$, the wake has evolved into a series of horseshoe-shaped vorticity structures with alternating regions of clockwise and counterclockwise vorticity.

Figure 4 shows the Fourier transform of the coefficient of lift for the Clark-Y airfoil simulation of Figure 3. The primary peak occurs at a period of about 4.3 units of nondimensional time, which corresponds to the observed period of vortex shedding in the simulation.

Experimental observations of a 10cm-chord Clark-Y airfoil in a wind tunnel with a flow speed of 21.5m/s showed that the primary component of the lift signal at high angles of attack has a frequency of about 40Hz [5]. This corresponds to a period of about 5.4 units of nondimensional time, which agrees roughly with our simulation.

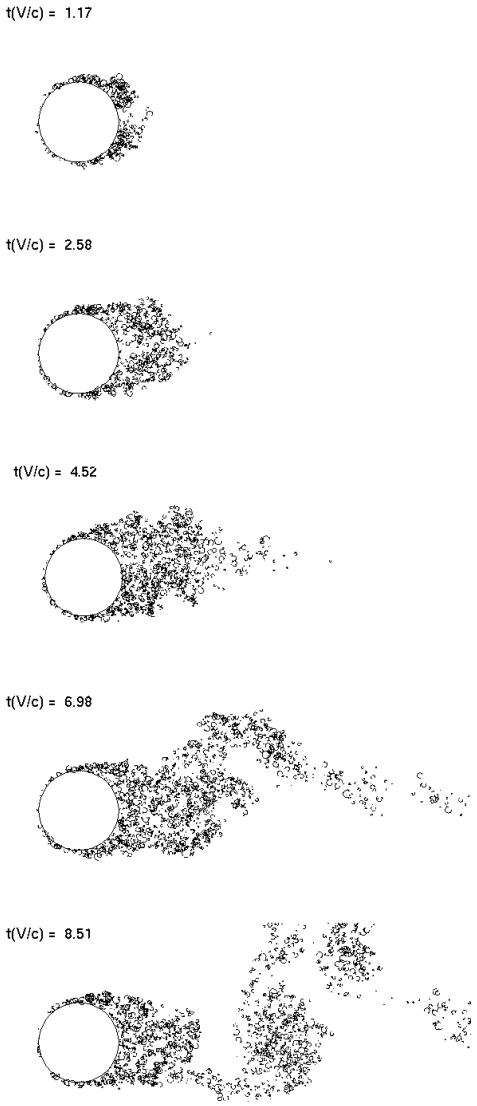

Figure 2: Simulation snapshots of flow past a cylinder accelerated instantaneously from rest. The small circular arcs represent point vortices, and the fluid flows from left to right. The first two pictures show the initial vorticity shedding and the development of a viscous wake. In the third view, a large mass of clockwise vorticity is separating from the wake. The fourth view shows two counter-rotating coherent structures, and the fifth shows a third forming in the wake.

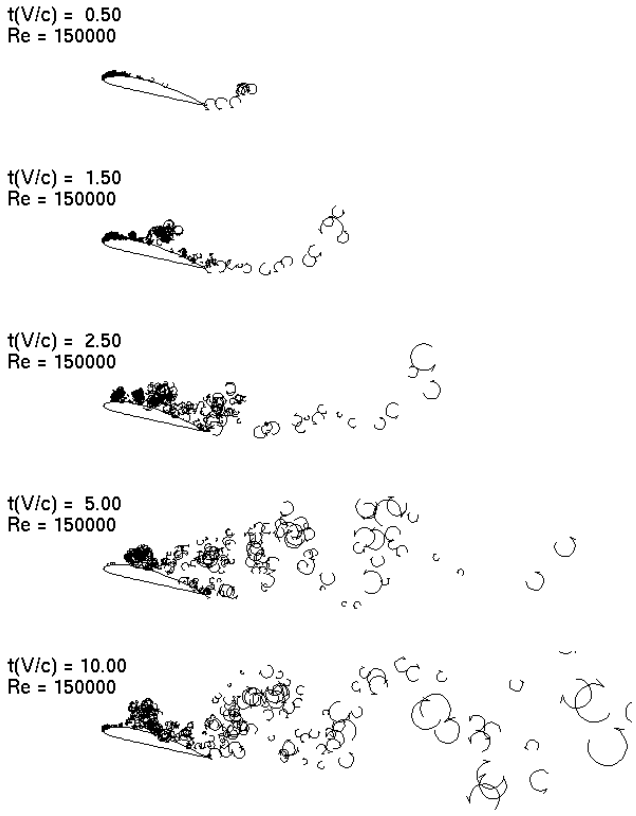

Figure 3: Simulation snapshots of flow past a Clark-Y airfoil at $\alpha = 0.25$rad.

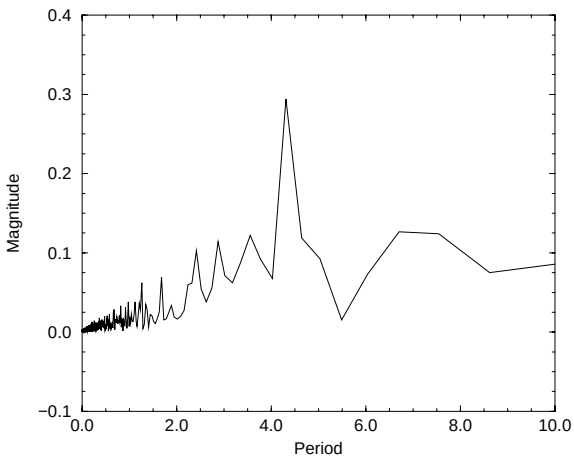

Figure 4: Fourier analysis of the lift signal for the Clark-Y airfoil at $\alpha = 0.25$rad.

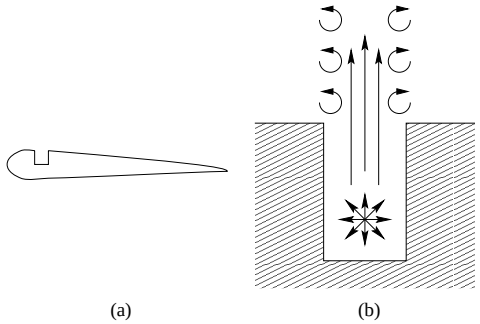

Figure 5: An abstraction of a jet actuator. (a) the placement of the actuator in the airfoil. (b) Close-up of the actuator. The point source at the bottom of the notch creates an upward flow, and the vortices shed from the walls of the notch keep the jet collimated.

4 Future work

4.1 Improving computational efficiency

As stated previously, the most computationally intensive task in evaluating this model is handling the vortex-vortex interactions. Under the current algorithm, the time required is $O(n \log n)$, where n is the number of vortices, because of the method of organizing vortices into clusters and simplifying intercations between clusters and distant vortices.

Further efficiency can be obtained by abstracting interactions between clusters as well, as described by Greengard and Rohklin [3]. This method has a computational load of $O(n)$, and is used by Koumoutsakos and Leonard in [4].

4.2 Simulating actuators

The ultimate goal of this work is to develop a theory of boundary control of flows using pulsed air injection. To that end, a means of modeling a pulsed-jet actuator is needed.

One possible model is shown in figure 5. The jet is simulated by a point source inside a notch in the airfoil surface. (A point source has complex potential $w = m/(2\pi)\log(z - z_0)$ where m is the source strength and z_0 is its location.) This combination results in a flow out the top of the notch. In an inviscid potential flow (i.e., no vortex shedding) such a flow would disperse in all directions at the notch opening. However, if the walls of the notch are treated as vortex-shedding surfaces (i.e., as ordinary panels of the airfoil surface) then vortices will escape the notch walls at the upper corners. These vortices will serve to shape the outflow into a jet, which is the appropriate physical result.

4.3 Investigating coherent structures

The qualitative features of the coherent vortex structures observed in the simulations agree with experiments. These structures are of fundamental importance to boundary flows. While we are a long way from having a complete theory of the formation of the coherent structures observed in both nature and our point-vortex simulations, it has not been difficult to obtain a number of striking results on the formation of patterns in low dimensional vortex systems. It is well known, for instance, that an infinite line of evenly spaced vortices of equal strength is an equilibrium for the point vortex dynamics discussed in Section 2.1. Similarly, a pattern of point vortices of equal strengths evenly distributed around the circumference of a circle is a *relative* equilibrium wherein the configuration remains a circle of fixed radius and constant rotation rate with the individual vortices remaining on the circle at a fixed distance from each other. What is surprising is that if n is the number of vortices, the circular relative equilibrium configuration is stable if and only if $n \leq 7$. Whether such qualitative results can be extended to the point where they illuminate the more difficult questions of how the coherent structures depicted in Figures 2 and 3 are formed and how they might be controlled (using the actuator models discussed above) is a goal of future research. Our goal is to develop a theoretical and computational basis for understanding how to organize pulsed-jet actuation to shape and control the dynamics of coherent structures. More specifically, our immediate aim is to develop a theory governing the type of flow control discussed in [5]. While all results to date have involved 2-d models (and hence 2-d effects), it may be necessary to account for three-dimensional effects in order to understand how pulsed jets actually influence the flow.

References

[1] J. E. Barnes and P. Hut. A hierarchical $O(N \log N)$ force-calculation algorithm. *Nature*, 1986.

[2] G. K. Batchelor. *Fluid Dynamics*. Cambridge University Press, 1967.

[3] L. Greengard and V. Rokhlin. A fast algorithm for particle simulations. *Journal of Computational Physics*, 1987.

[4] P. Koumoutsakos and A. Leonard. High-resolution simulations of the flow around an impulsively started cylinder using vortex methods. *Journal of Fluid Mechanics*, 1995.

[5] S. H. Lee. Control of boundary layer separation using pulsed jet actuators. Master's thesis, Boston University, September 1998.

[6] H. Lin, M. Vezza, and R. A. M. Galbraith. Discrete vortex method for simulating unsteady flow around pitching aerofoils. *AIAA Journal*, 35(3):494–499, 1997.